FORMATION OF GALACTIC BULGES

NICKOLAY Y. GNEDIN,[1] MICHAEL L. NORMAN,[2] AND JEREMIAH P. OSTRIKER[3]

ABSTRACT

We use cosmological hydrodynamic simulations to investigate the formation of galactic bulges within the framework of hierarchical clustering in a representative cold dark matter (CDM) cosmological model. We show that the largest objects forming at cosmological redshifts $z \sim 4$ resemble observed bulges of spiral galaxies or moderate-sized ellipticals in their general properties, such as size, shape, and density profile. This is consistent with observational data indicating the existence of "old" bulges and ellipticals at more moderate redshifts. These bulges are gas dominated at redshift $z = 3$, with high rates of star formation, and would appear to be good candidates for small blue galaxies seen in the Hubble Deep Field.

Subject headings: cosmology: theory — galaxies: formation — intergalactic medium — large-scale structure of universe

1. INTRODUCTION

The fact that bulges of ordinary galaxies (and indistinguishable ellipticals of the same luminosity) are very dense is often used as an argument against the currently favored cold dark matter (CDM)–type cosmological models. Really, since the average density of the universe decreases with time, and the average density of a bound object is directly proportional to the density of the universe at the time at which the object is formed, dense galactic bulges should have formed at very high redshift. Thus, it is reasonable to ask whether currently fashionable cosmological models normally have enough small-scale power to account for the formation of massive (10^9–10^{10} $M_\odot$ in baryons) bulges at $z \gtrsim 10$ (Peebles 1997).

This argument can be illustrated by the following simple estimate: the characteristic number density of baryons in the Galactic bulge within a sphere of radius 3 kpc is

$$n_{GB} \sim 2 \text{ cm}^{-3} \quad (1)$$

(Kent, Dame, & Fazio 1991; Freudenreich 1998). In comparison, the average density of the cosmological virialized object formed at redshift z is only

$$n_{TH} \sim 10^{-4}(1 + z)^3 \text{ cm}^{-3} \quad (2)$$

for $\Omega_b h^2 = 0.02$, and we assume that the average density of the virialized object is about 200 times the average density of the universe at the moment of formation (Gunn & Gott 1972), according to the standard dissipationless collapse theory. Comparing equations (1) and (2), we can deduce that the bulge of our Galaxy formed at $z_{GB} \sim 30$. However,, none of the currently acceptable CDM-type models can form 10^{10} $M_\odot$ baryonic objects at $z = 30$ in numbers even closely comparable to the observed number density of galactic bulges.

Does this argument imply that the CDM-type models are ruled out? We try to show in this paper that the answer to this question is no. What this simple argument misses is the ability of baryons to cool and collapse to densities exceeding that of the dark matter. We present a series of cosmological hydrodynamic simulations that include adequate physical modeling to properly account for the formation of bulges of galaxies, and we show that typical bulges form in a realistic CDM-type model at $z \sim 5$ rather than at $z \sim 30$.

But before describing our detailed results, it is perhaps worth noting the conceptual flaw in the simple argument we first presented. The global ratio of baryons to dark matter in our simulation and in typical current estimates is about 1:8. However, in our own galactic bulge the baryonic (stellar) component exceeds the dark matter component and perhaps by as much as a factor of a few. Thus (taking the cube root of density enhancement), the baryonic stellar component has contracted relative to the dark matter component by a factor of 2–4 and, correspondingly, the bulge should have formed in the plausible redshift range of $z \sim 5$–10 rather than at $z = 30$. Furthermore, as we shall see, the observed (and computed) profiles are very different from those envisioned in the top-hat collapse picture.

An aside on a related but quite different problem may be useful here. There is currently a good deal of discussion on the subject of whether or not standard CDM models make bulges that are *too* dense (e.g., Spergel & Steinhardt 1999; Burkert & Silk 1999; Moore et al. 1999; Kravtsov et al. 1998). However, these papers address far lower mass systems and ones that are dark matter dominated, having circular velocities of less than 100 km s^{-1}. Here we address normal bulges with (equivalent) circular velocities of about 200 km s^{-1} or more, for which the advertised problem has been the opposite: why are they *so* dense?

Some work on the subject has been done by Steinmetz & Mueller (1994, 1995). However, they modeled the formation of disk galaxies as the collapse of an isolated gas cloud, whereas in this work we consider the formation of galactic bulges within the framework of hierarchical clustering, based on realistic cosmological simulations that include such effects as the cosmological infall, merging of protogalactic clumps, and expansion of the universe, all of which are missing in Steinmetz & Mueller's work. Other numerous numerical investigations of galaxy formation do not

[1] Center for Astrophysics and Space Astronomy, University of Colorado, Boulder, CO 80309; gnedin@casa.colorado.edu.

[2] Laboratory for Computational Astrophysics, National Center for Supercomputing Applications, University of Illinois at Urbana-Champaign, 405 North Matthews Avenue, Urbana, IL 61801; norman@ncsa.uiuc.edu.

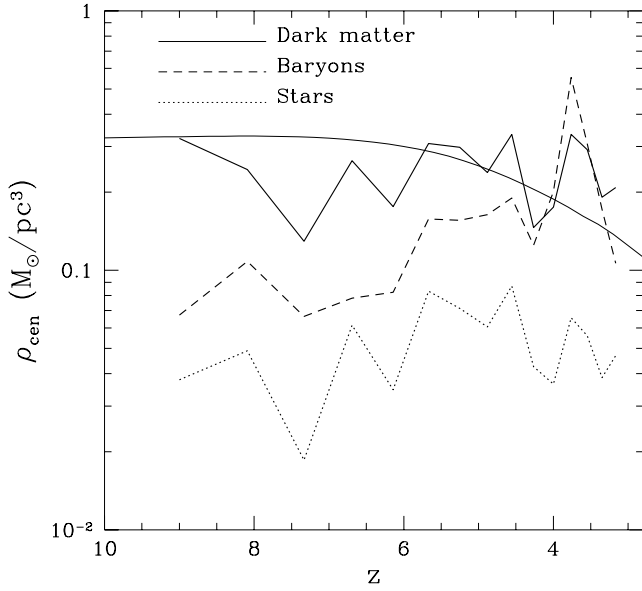[3] Princeton University Observatory, Peyton Hall, Princeton, NJ 08544; jpo@astro.princeton.edu.

FIG. 1.—Evolution of the central dark matter density (*solid lines*), baryonic density (*dashed lines*), and stellar density (*dotted lines*) for the most massive object in our simulation. The thin solid line shows the central total density of the same object if it had the Navarro-Frenk-White (NFW) density profile. The central core appears because of finite spatial resolution in simulations.

specifically concentrate on the bulges, or lack the mass and/or spatial resolution to say anything about bulge formation.

2. SIMULATIONS

We use the softened Lagrangian hydrodynamics (SLH) cosmological hydrodynamic code (Gnedin 1995, 1996; Gnedin & Bertschinger 1996). Physical modeling included in the code is fully described in Gnedin & Ostriker (1997). We choose a CDM + Λ cosmological model with the cosmological parameters

$$\Omega_0 = 0.37 , \quad \Omega_L = 0.63 , \quad h = 0.70 , \quad \Omega_b = 0.049 ,$$

which is close to the "concordance" model of Ostriker & Steinhardt (1995) and to models that are consistent with recent supernova Type Ia (SN Ia) results (Riess et al. 1998; Perlmutter et al. 1999). We have performed one simulation with 128^3 baryonic resolution elements, the same number of dark matter particles, and a number of stellar particles were formed during the simulation. The simulation box size was fixed to 3 h^{-1} Mpc, which resulted in a total mass resolution of 1.3×10^6 h^{-1} $M_\odot$. For reference, the Jeans mass at $z = 10$ and $T = 10^4$ K is about 10^{10} h^{-1} $M_\odot$. The spatial resolution was fixed at 1.5 h^{-1} comoving kpc. Because of the small box size, this simulation cannot be
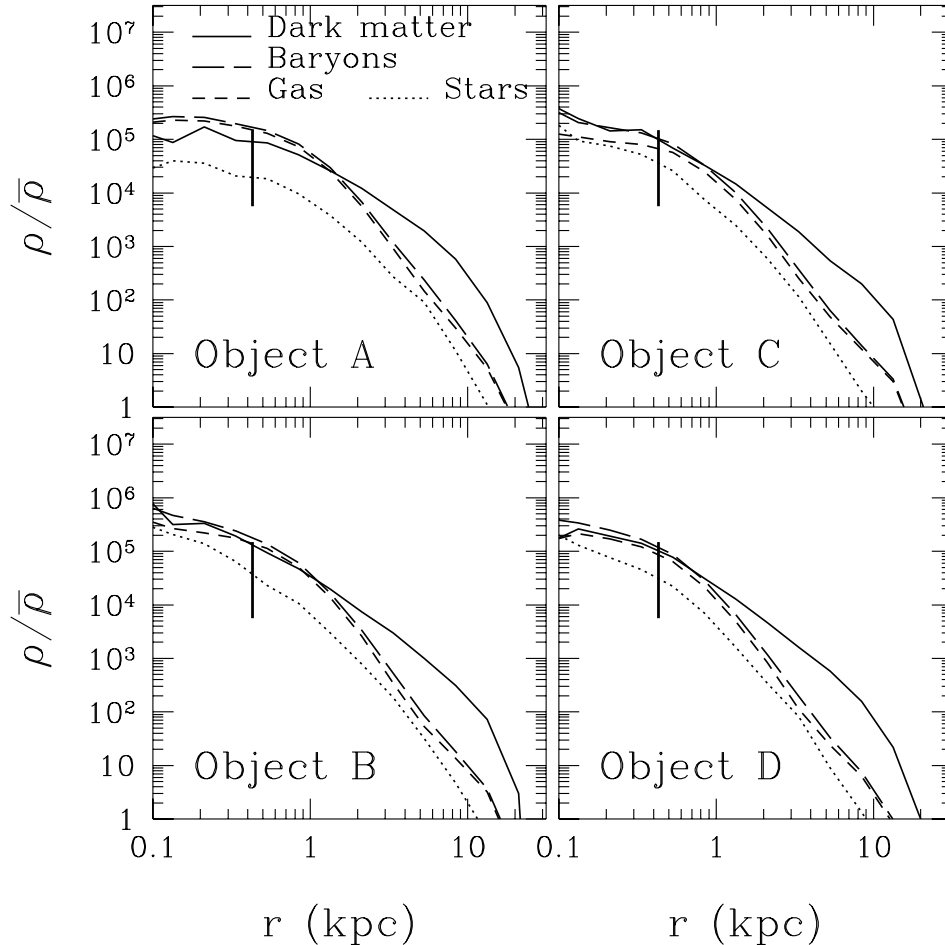

FIG. 2.—Density profiles for the dark matter (*solid lines*), total baryons (gas and stars, *dashed lines*), and stars (*dotted lines*) of the four most massive objects at $z = 3.8$ as a function of radius in physical (not comoving) units. The bold vertical bar marks the spatial resolution of the simulation (450 pc).
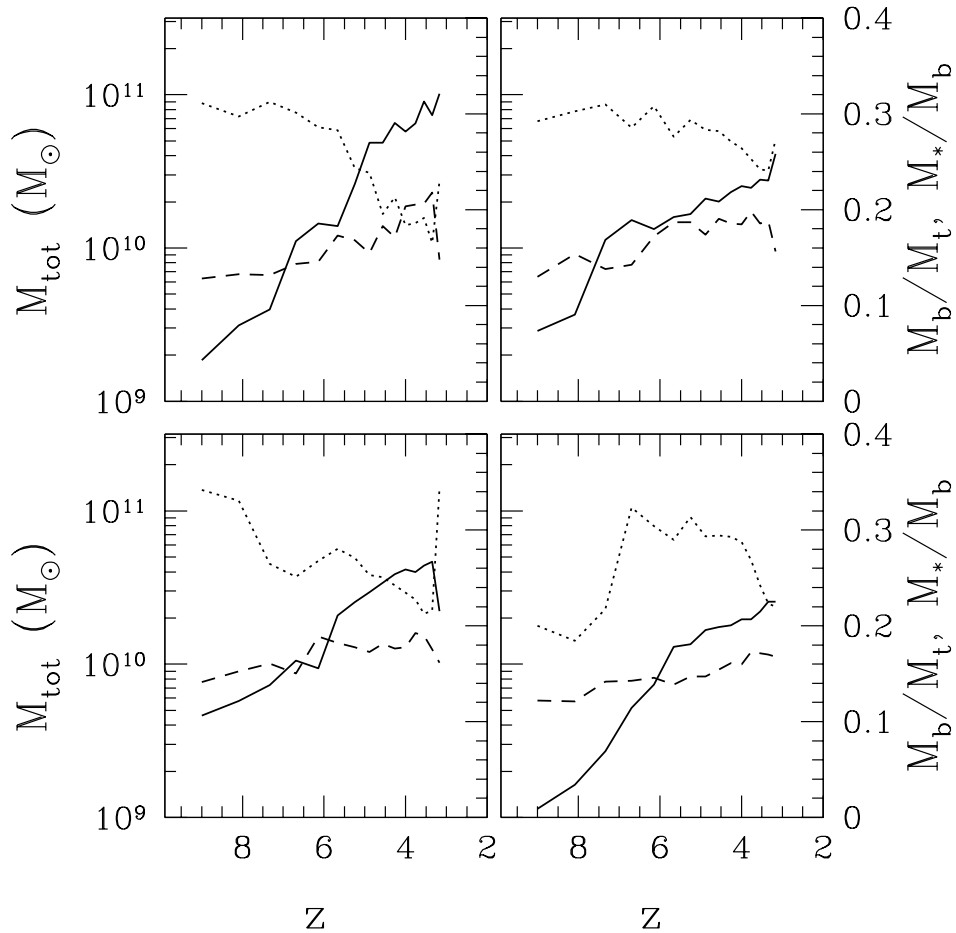
FIG. 3.—Evolution of the total mass (*solid lines*), baryonic fraction (*dashed lines*), and stellar fraction (per unit baryonic mass, *dotted lines*) of the four most massive objects.

continued to $z = 0$. Instead, we stopped the simulation at $z \approx 3$.

Even at this redshift, our simulation suffers from a lack of spatial of resolution, as is illustrated by Figure 1, which shows the evolution of the central density for the dark matter, baryonic, and stellar components of the most massive object from our simulation. The central density is defined as the average density within the sphere of two resolution lengths of our simulations (~ 900 pc at $z = 3.8$). As an illustration, we also show the central density of the Navarro, Frenk, & White (NFW) profile, which is defined in the same way and is therefore a function of resolution (and thus time, since we keep the resolution fixed in the comoving coordinates)—as redshift decreases, so does our spatial resolution in the physical coordinates. The fact that the NFW density actually starts to decrease for $z < 6$ indicates that our resolution becomes comparable to the characteristic radius of the object—the radius at which the local density slope approaches -2.

Another simulation with 8 times more resolution elements (256^3) and a 6 h^{-1} Mpc box was also performed. The large simulation thus had the same mass resolution as the small one, and the spatial resolution in the large simulation was fixed at 1.2 h^{-1} comoving kpc. However, because the large simulation required a computational expense beyond what was available to us, it was terminated at $z = 9.5$. Thus, we use the large simulation to verify numerical convergence and estimate missing small scale power, but we use the small (128^3) simulation as the source for scientific results.

By comparing the large and small simulations, we have found that the small simulation included most of the small-scale power that was initially present in the baryonic component. Thus, our results are not significantly affected by the finite resolution in the initial conditions (k-space resolution), but they are, of course, subject to finite mass and spatial resolution.

3. RESULTS

Since we are concerned with the formation process of galactic bulges and small ellipticals, we focus in this paper on properties of individual objects formed in our simulations. Specifically, we focus on the four most massive objects. Each of these objects contains more than 10,000 particles of each kind (i.e., dark matter, gas, and stars), and thus they are fully resolved numerically.

Tables 1 and 2 present the general properties of the four objects: their total, baryonic, and stellar masses, as well as the ratio of the baryonic to the total mass, and the stellar to the baryonic mass at $z \approx 4$ and $z \approx 3$, respectively.

A few observations can easily be made from the table. First, the objects contain more baryons than the cosmic average of $\Omega_b/\Omega_0 = 0.13$. Second, they are still dominated by gas, since only about 20%–30% of their baryonic mass is turned into stars when we terminated the computation at $z \approx 3$. These objects have a moderately high rate of star formation (several $M_\odot$ yr^{-1}), and would appear to correspond well to the numerous small blue objects seen in the
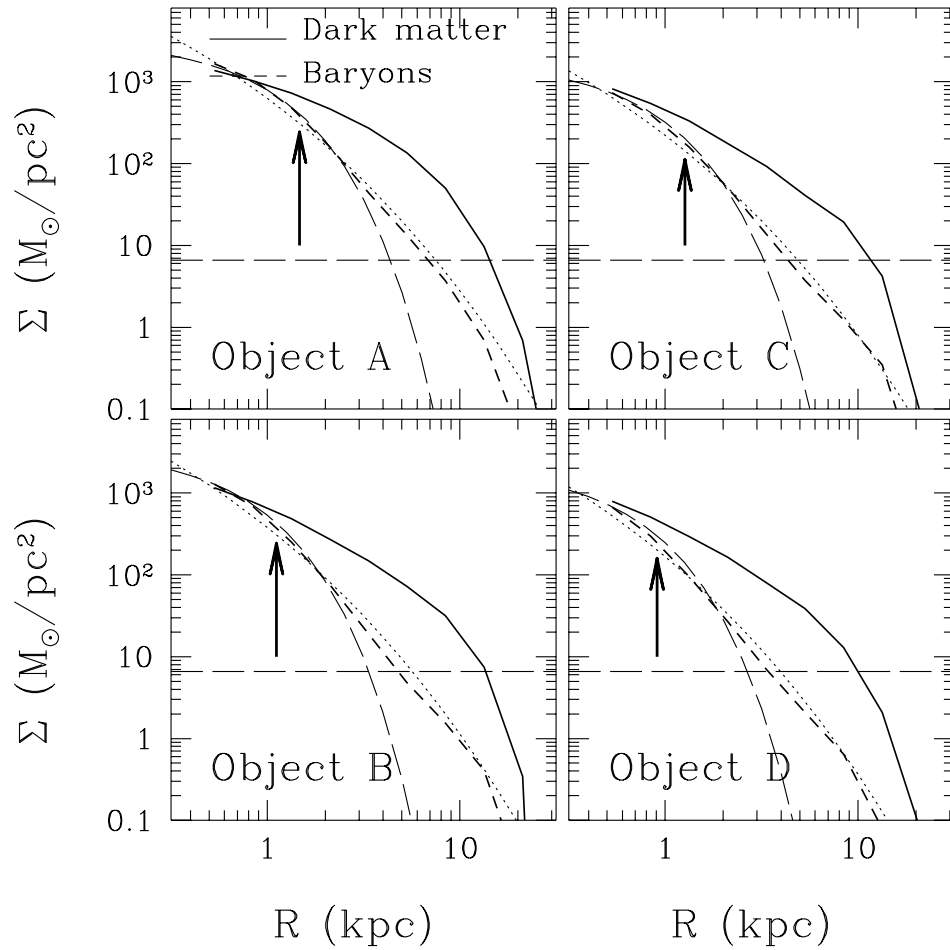
FIG. 4.—Surface mass density profiles for the dark matter (*solid lines*) and total baryons (*dashed lines*) of the four most massive objects at $z = 3.8$ as a function of radius in physical (not comoving) units. The profiles are terminated at the resolution limit of the simulation (450 pc). Tilted long-dashed lines show a $r^{1/4}$ law for the baryonic profiles, and dotted lines show exponential profiles. Bold arrows show characteristic radii, R_e, for $r^{1/4}$ profiles. The horizontal long-dashed line show the central surface density of a homogeneous top-hat sphere.

Hubble Deep Field (Contardo, Steinmetz, & Alvensleben 1998).

However, it must be noted here that the amount of gas turned into stars really depends on the specifics of the star

TABLE 1

FOUR MOST MASSIVE OBJECTS AT $z = 4$

Object	Total Mass ($M_\odot$)	Baryonic Mass ($M_\odot$)	Stellar Mass ($M_\odot$)	M_b/M_t	M_*/M_b
A	4.0×10^{10}	8.2×10^9	1.5×10^9	0.20	0.18
B	2.9×10^{10}	5.1×10^9	1.2×10^9	0.18	0.23
C	1.8×10^{10}	3.3×10^9	0.9×10^9	0.18	0.26
D	1.4×10^{10}	2.2×10^9	0.6×10^9	0.16	0.29

TABLE 2

FOUR MOST MASSIVE OBJECTS AT $z = 3$

Object	Total Mass ($M_\odot$)	Baryonic Mass ($M_\odot$)	Stellar Mass ($M_\odot$)	M_b/M_t	M_*/M_b
A	7.1×10^{10}	1.1×10^{10}	2.4×10^9	0.15	0.23
B	2.9×10^{10}	4.5×10^9	1.2×10^9	0.16	0.27
C	1.8×10^{10}	3.0×10^9	0.9×10^9	0.17	0.22
D	1.6×10^{10}	2.5×10^9	0.9×10^9	0.16	0.34

formation algorithm adopted in the simulation. We make no pretense that we can fully account for the star formation in our simulations; it is clear that the modeling of star formation needs to be much more advanced before simulations can claim to predict the star formation rate in (proto) galaxies with sufficient detail. Thus, for the purpose of this paper we will pay little attention to the stellar component of our simulated bulges, and instead focus primarily on the total baryonic component. We assume that with the proper star formation algorithm, our simulated bulges will form stars at an appropriate rate as long as the total baryonic distribution is compatible with observations.

Since at $z < 3.8$ our results become substantially contaminated by the lack of spatial resolution, we will restrict most of our analysis to $z = 3.8$, the lowest redshift at which characteristic radii of bound objects are still well resolved. Density profiles of the four most massive objects are shown in Figure 2. The most massive object, object A, is less dense at the center than the other three objects because it experienced a major merger shortly before $z = 4$ and has not yet fully relaxed. Object D has also experienced a major merger at $z \approx 6$, whereas objects B and C have been accreting matter quietly since $z \sim 10$. We point out here that in all four objects, baryonic density at the center is greater than or similar to the dark matter density, i.e., baryons in all four
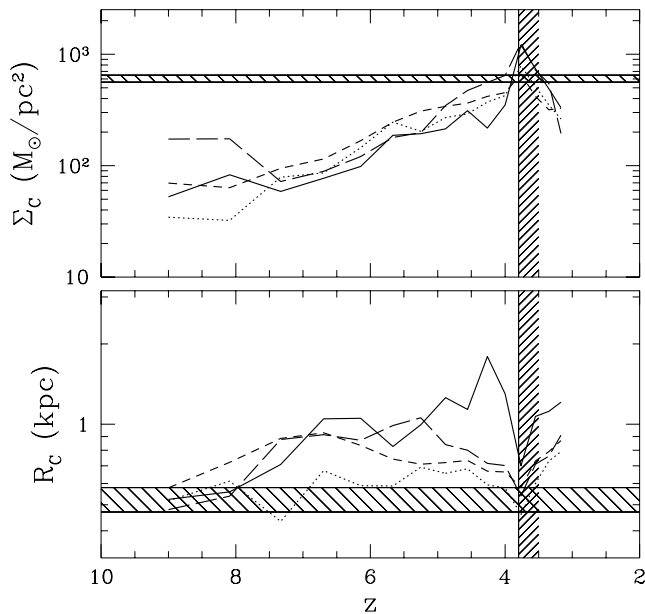
FIG. 5.—Evolution of the characteristic radii (*bottom*) and densities (*top*) for the four objects: A (*solid lines*), B (*long-dashed lines*), C (*short-dashed lines*), and D (*dotted lines*). The horizontal shaded areas mark the range of values for the Galactic bulge, and the vertical line marks the boundary $z = 3.8$ beyond which our simulation fails to resolve cores of the galactic bulges.

objects are self-gravitating. As an aside, we note that should the gaseous component dominate at the center at any time, a rapid collapse would occur, which presumably would be accompanied by rapid star formation or, should a black hole of sufficient mass be present, the concomitant flare-up of an active galactic nucleus (AGN). Clearly, we do not have sufficient resolution to follow this phase (but see Abel, Bryan, & Norman 1999).

Evolution of the average properties of these objects is shown in Figure 3. One can immediately see that all four objects are experiencing heavy merging at $z \sim 4$–6, increasing their mass by about an order of magnitude. The stellar fraction of object A decreased significantly at $z = 4$–5 because of the accretion of a large quantity of fresh gas. Also noticeable is the increase in the total baryonic fraction in object A at $z \sim 4$. Since baryons are almost self-gravitating at the center of object A, they efficiently cool and collapse toward the center, leading to the increase in the baryonic fraction of the object.

Figure 1 shows the evolution of the central density for the dark matter, baryonic, and stellar components of object A. One can see that the dark matter density does not change systematically with time (albeit fluctuating significantly) until the lack of resolution contaminates the results, because the object is close to the virial equilibrium. On the contrary, the baryonic density increases with time because
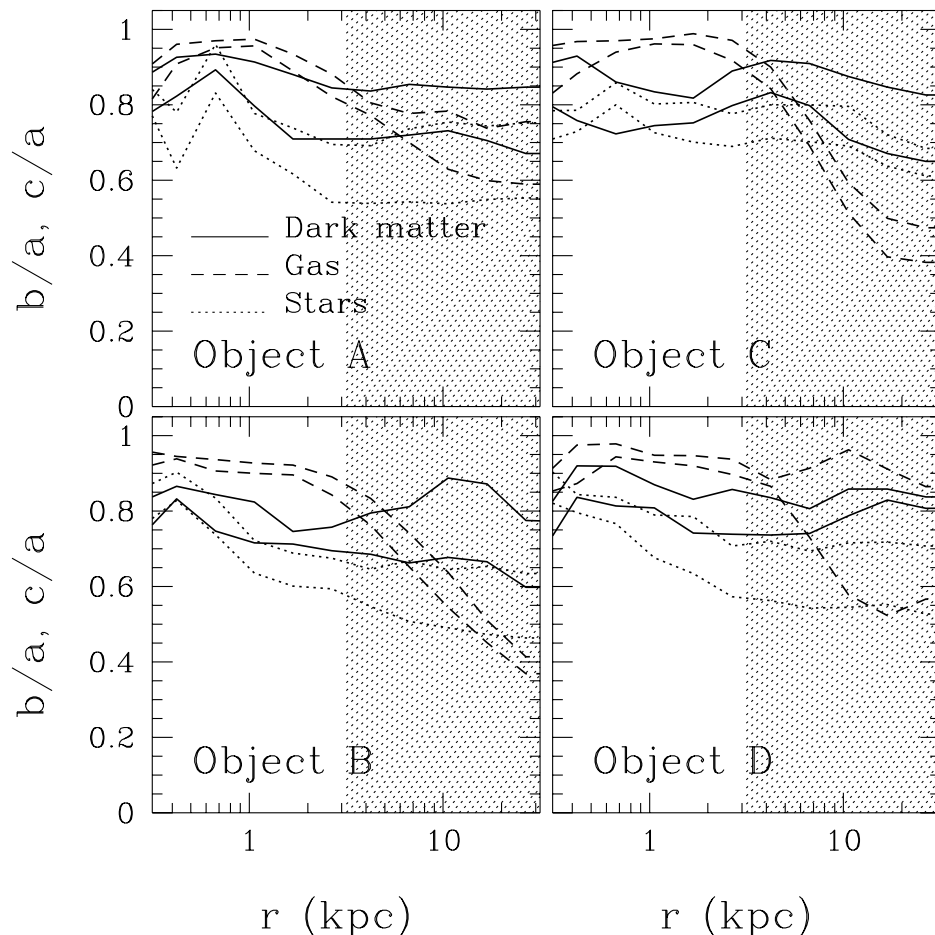

FIG. 6.—Axis ratios for the dark matter (*solid lines*), total baryons (gas and stars, *dashed lines*), and stars (*dotted lines*) of the four most massive objects at $z = 3.8$ as a function of radius in physical (not comoving) units.
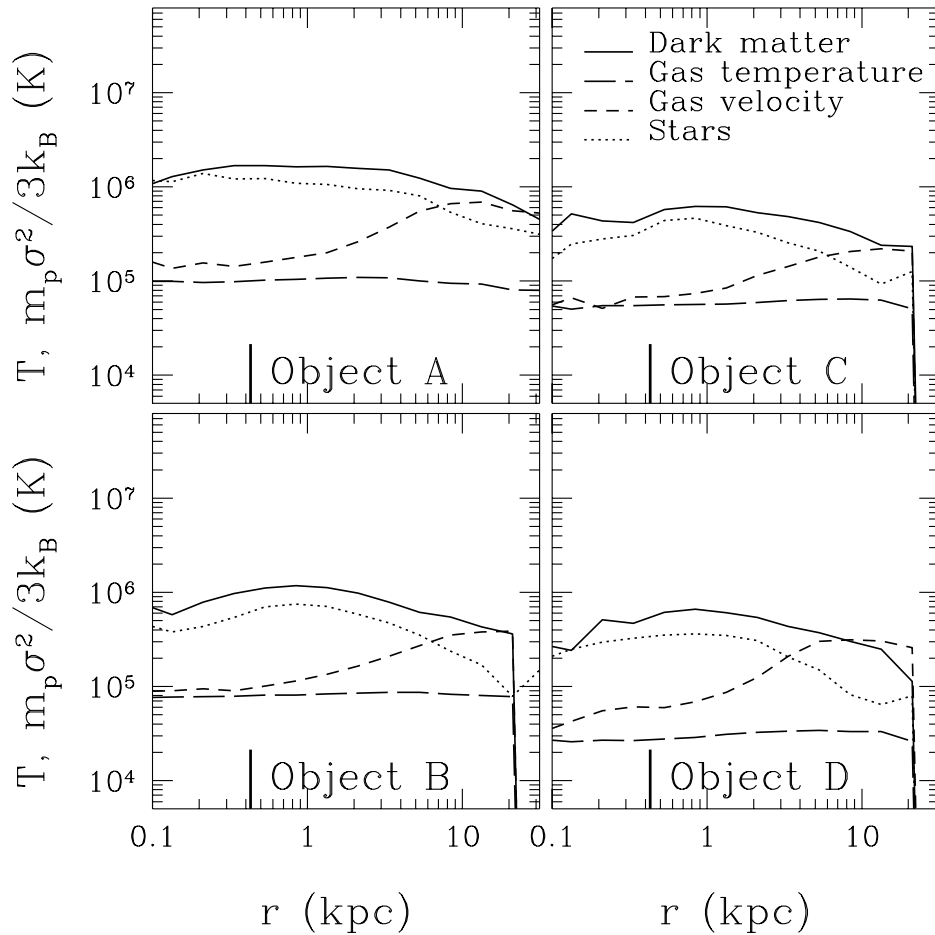
FIG. 7.—Velocity dispersion and gas temperature profiles for the four most massive objects at $z = 3.8$. Shown are the dark matter velocity dispersion (*solid lines*), gas temperature (*long-dashed lines*), gas velocity dispersion (*short-dashed lines*), and stellar velocity dispersion (*dotted lines*). The velocity dispersions are converted into temperature units.

of efficient cooling at the center of the object. The recent merger at $z \sim 5$ triggered a considerable increase in the central density of gas, but this increase has not yet resulted in the burst of star formation. We expect that if we continued the simulation to lower redshift with higher spatial resolution, object A would experience a burst of star formation at the center, which would transform most of the gas into stars on a rather short timescale.

We are now ready to address the major question of this paper: do those objects formed in the simulation resemble real galactic bulges? In order to answer this question, we show in Figure 4 the surface density profiles for our four objects. In addition, for the total baryonic profile we compute the exponential fits in the form

$$\Sigma(R) = \Sigma_C \, e^{1 - R/R_C} , \qquad (3)$$

and $r^{1/4}$ law fits,

$$\Sigma(R) = \Sigma_e \, 10^{-3.3307[(R/R_e)^{1/4} - 1]} . \qquad (4)$$

As can be seen from Figure 4, the central 3 kpc of the simulated bulges are equally well fitted by both the exponential and the de Vaucouleurs profiles, and we lack the resolution to distinguish them at the very center. We also note that our resolution is barely enough to resolve the characteristic scales of the two profiles, so we may overestimate the characteristic radii somewhat, but not by a large

factor. However, both the Kent, Dame, & Fazio (1991) and Freudenreich (1998) models for the galactic bulge are well fitted by the exponential profile for the range $0.1 < r < 3$ kpc (with respective rms errors of 3% and 8%, respectively), and thus agree with our simulations over the range of scales that we can resolve.

We put together the parameters of the fits in Table 3. In addition, we list the parameters that describe the Galactic bulge from Kent, Dame, & Fazio (1991) and Freudenreich (1998), for comparison. As one can see, objects that we

TABLE 3
FIT PARAMETERS FOR THE FOUR MOST MASSIVE OBJECTS AT $z = 3.8$

Object	R_C (kpc)	Σ_C ($M_\odot$ pc^{-2})	R_e (kpc)	Σ_e ($M_\odot$ pc^{-2})
A	0.70	1200	1.47	310
B	0.54	1270	1.11	310
C	0.58	664	1.27	140
D	0.46	790	0.91	200
Galactic bulge[a]	0.58	650[c]	0.97	250[c]
Galactic bulge[b]	0.47	560[c]	0.76	260[c]

[a] Kent et al. 1991.
[b] Freudenreich 1998.
[c] A mass-to-light ratio of 3 is assumed in converting luminosity to mass.

observe in the simulation are very similar to (or perhaps even a little bit larger than) the bulge of Milky Way, provided that they convert most of their gas into stars.

Why did we then erroneously conclude in § 1 that the CDM-type models predict too low density bulges? The answer to this puzzle is again illustrated in Figure 4. The horizontal long-dashed line in that figure shows the central surface density for a homogeneous top-hat sphere, i.e., for a spherical object with a constant density 200 times the average density of the universe and with a radius equal to the virial radius of object A (all four objects have quite similar virial radii). One can immediately see that the top-hat model underestimates the central density of an object by about 2 orders of magnitude. Even the density at the characteristic radii (R_C, R_e) is 30–100 times greater than the fiducial top-hat virial density.

The evolution of the two fit parameters, the characteristic radius and density, is shown in Figure 5 for the four most massive objects in the simulation. The densities increase steadily as the gas continues to accrete and cool inside the dark matter halos, whereas characteristic radii stay approximately constant for all objects.

Finally, if we want to demonstrate that we can form galactic bulges in a realistic cosmological simulation, we should address the question of the bulge shape. The bulge of our Galaxy is quasi-spherical, or, at the very least, slightly ellipsoidal. Is this shape also reproduced in the simulation? Figure 6 addresses this question. In it we show the axis ratios for the dark matter, gas, and stars for our four objects as a function of radius. One can see that in the central parts, the gas and stellar distributions are quite close to spherical. Shapes at larger radii, $r > 3$ kpc, shown shaded in Figure 6, vary significantly among all the objects, but at those large distances the gas is far from equilibrium, and the minute shape of its distribution has little relation to its final state. The fact that the objects we observe in the simulation are more-or-less spherical, rather than disk-shaped, is due to the fact that at high redshift the slope of the linear power spectrum of the density fluctuations is close to -3. This results in a range of scales becoming nonlinear almost at the same time, which in turn leads to heavy merging among the objects observed in the simulation. Thus, gaseous disks do not have enough time to form, and the shape of the objects remains quasi-spherical. Only at later times, when the rate of merging falls, can a gaseous disk form inside an object.

In order to confirm this claim, in Figure 7 we show the velocity dispersion and temperature profiles for the four objects mentioned above. As one can see, the gas velocity dispersion is somewhat larger than the gas temperature, and so the turbulent motions in the gas provide more than 50% of the support against gravity. Because the molecular and/or magnetic viscosity is not large on the scales that we can resolve, it would take some time before the gas can settle into a rotationally supported disk. Thus, in order for our objects to resemble stellar bulges at the present epoch, the turbulence dumping time should be large compared to the star formation time.

4. CONCLUSIONS

We have showed that objects that form in a realistic cosmological simulation of a CDM-type cosmological model do look similar to bulges of normal galaxies. Our objects are still 75% gaseous at $z \approx 4$, but they form stars at a high rate, and most of the gas in those objects will be converted into stars by redshift $z = 2$. In this time frame they resemble the numerous small blue galaxies seen in the HDF. The number density of such objects predicted from our simulation is about a factor of 2 larger than the actual number observed in the HDF and Lyman-break (LBG) galaxy samples (Steidel et al. 1999); however, a precise comparison with observations depends crucially on (highly uncertain) assumptions about the star formation, and is not possible at present. Later, the simulated objects will look like slightly ellipsoidal stellar objects, with the density profiles well fitted by the exponential profile and with the parameters of the fit similar to the parameters of the Milky Way bulge and small elliptical galaxies.

We thus conclude that currently favorable CDM-type cosmological models have no difficulty in reproducing observed properties of galactic bulges. On the contrary, models that have galaxy formation at $z \sim 30$ (Peebles 1997) would form bulges that are 2–3 orders of magnitude denser than the observed ones. This conclusion is further boosted by the consideration that, due to the limited mass and spatial resolution of our simulation, we can only *underpredict* the densities and masses of cosmological objects. With several bulges observed in an approximately correct mass range (note the Local Group with M31, M33, and the Galaxy), and a total luminosity of about L_* in the volume of 27 h^{-3} Mpc^3, we conclude that the model produces approximately the correct density of bulges.

REFERENCES

Abel, T., Bryan, G. L., & Norman, M. L. 1999, in Evolution of Large-Scale Structure: from Recombination to Garching, ed. A. J. Banday et al. (Enschede: PrintPartners), 42
Burkert, A., & Silk, J. 1999, in Dark Matter in Astrophysics and Particle Physics 1998, ed. H. V. Klapdor-Kleingrothaus (Bristol: Institute of Physics), 375
Contardo, G., Steinmetz, M., & Alvensleben, U. F. 1998, ApJ, 507, 497
Freudenreich, H. T. 1998, ApJ, 492, 495
Gnedin, N. Y. 1995, ApJS, 97, 231
———. 1996, ApJ, 456, 1
Gnedin, N. Y., & Bertschinger, E. 1996, ApJ, 470, 115
Gnedin, N. Y., & Ostriker, J. P. 1997, ApJ, 486, 581
Gunn, J. E., & Gott, J. R. 1972, ApJ, 176, 1
Kent, S. M., Dame, T. M., & Fazio, G. 1991, ApJ, 378, 131

Kravtsov, A. V., Klypin, A. A., Bullock, J. S., & Primack, J. R. 1998, ApJ, 502, 48
Moore, B., Ghigna, S., Governato, F., Lake, G., Quinn, T., Stadel, J., & Tozzi, P. 1999, ApJ, 524, L19
Ostriker, J. P., & Steinhardt, P. J. 1995, Nature, 377, 600
Peebles, P. J. E. 1997, ApJ, 483, L1
Perlmutter, S., et al. 1999, ApJ, 517, 565
Riess, A. G., et al. 1998, AJ, 116, 1009
Spergel, D. N., & Steinhardt, P. J. 1999, Phys. Rev. Lett., 84, 3760
Steidel, C. C., Adelberger, K. L., Giavalisco, M., Dickinson, M., & Pettini, M. 1999, ApJ, 519, 1
Steinmetz, M., & Mueller, E. 1994, A&A, 281, 97
———. 1995, MNRAS, 276, 549